REPORT DOCUMENTATION PAGE

Form Approved
OMB No. 0704-0188

1. REPORT DATE (DD-MM-YYYY)	2. REPORT TYPE	3. DATES COVERED (From - To)
09-March-2005	Final Technical	xxxxxxxxx - 09.30.04

4. TITLE AND SUBTITLE

System for bulk growth of Gallium Nitride

Vapor Phase Epitaxy of Gallium Nitride by Gallium Arc Evaporation

5a. CONTRACT NUMBER

5b. GRANT NUMBER
F49620-03-1-0235

5c. PROGRAM ELEMENT NUMBER

6. AUTHOR(S)
Dr. Sten J. Heikman, Dr. Umesh K. Mishra

5d. PROJECT NUMBER

5e. TASK NUMBER

5f. WORK UNIT NUMBER

7. PERFORMING ORGANIZATION NAME(S) AND ADDRESS(ES)
University of California, Santa Barbara CA 93106

8. PERFORMING ORGANIZATION REPORT NUMBER

9. SPONSORING / MONITORING AGENCY NAME(S) AND ADDRESS(ES)
Dr. Gerald L. Witt
AF Office of Scientific Research
4015 Wilson Blvd RM 713
Arlington, VA 22203-1954

10. SPONSOR/MONITOR'S ACRONYM(S)

11. SPONSOR/MONITOR'S REPORT NUMBER(S)

12. DISTRIBUTION / AVAILABILITY STATEMENT

Distribution Statement A: unlimited

AFRL-SR-AR-TR-07-0083

13. SUPPLEMENTARY NOTES

14. ABSTRACT

A vapor phase growth system intended for the growth of bulk gallium nitride crystals was investigated. Potential advantages of the growth technique are cheap source materials of high purity, no corrosive gasses, and low operating and equipment costs.

Ga contained in a crucible was evaporated by an arc discharge between a W-electrode and the Ga surface, and was transported to the growth zone by a carrier gas flowing over the Ga source. After mixing with ammonia, the mixture was passed between a top and a bottom susceptor, on which samples were mounted. High growth rates as high as 30 μm/hr were obtained on the top sample. The surface of deposited material was rough near the front of the susceptor, but was specular elsewhere and showed step-flow growth morphology in atomic force microscopy. The bottom sample experienced lower growth rates and a high density of macroscopic defects, presumably caused by Ga droplets in the gas phase.

Computer flow dynamic simulations predicted growth rates ~ 4 times higher than experiments. The discrepancy was attributed to ammonia pre-reactions, based on the experimental growth rate dependence on ammonia partial pressure. An additional factor 4 reduction in efficiency was due to Ga wall condensation between the evaporation and growth zones. The overall growth efficiency was 2 %.

15. SUBJECT TERMS

16. SECURITY CLASSIFICATION OF:			17. LIMITATION OF ABSTRACT	18. NUMBER OF PAGES	19a. NAME OF RESPONSIBLE PERSON
a. REPORT	b. ABSTRACT	c. THIS PAGE			Dr. Umesh K. Mishra
UNCLASSIFIED	UNCLASSIFIED	UNCLASSIFIED	UL	16	19b. TELEPHONE NUMBER (include area code) (805)893-3586

1 Background and Motivation

At present time, high quality GaN substrates are not commercially available. (Al,In)GaN based devices are fabricated from layer structures deposited on foreign substrates, including sapphire, SiC, and Si. The heteroepitaxy of GaN on these substrates leads to extended defects (dislocations) in the films, which are harmful in many device applications, affecting the device lifetime and performance. The lack of a GaN substrate has since the start of GaN research been considered one of the main technological obstacles. Commercialization of a GaN substrate will have an enormous impact on many facets of nitride semiconductor technology, in particular optoelectronic devices such as laser diodes and high performance LED chips.

High pressure growth techniques have been utilized to growth bulk GaN crystals, but the small size of the crystals obtained, the slow growth rate, and the high pressures involved suggest that these techniques are not suitable for commercial production.

Other candidates for bulk growth techniques include hydride vapor phase epitaxy (HVPE), sandwich sublimation, and more. However, to the best of our knowledge stable sustained growth rates well above 100 μm/hr are difficult to achieve, which renders the techniques impractical for large-scale bulk growth purposes. We believe a stable growth rate of at least 1 mm/hr over an area of 2" diameter will be necessary for commercial production. Several companies (Cermet, Kyma Technologies, TDI inc, and Cree) are currently developing GaN bulk growth technologies based on proprietary physical vapor transport techniques, vapor phase techniques, or traditional HVPE, but the potential of their technologies and products is presently unclear.

Recently, GaN 'pseudo' substrates grown by HVPE have become commercially available. These substrates consist of thick GaN films (10-100μm) deposited on a foreign substrate, and in some cases the substrate is removed. The high GaN film thickness leads to a reduced dislocation density, down to about 1×10^7 cm^{-2}. Epitaxial lateral overgrowth techniques can be applied to further reduce the dislocation density for applications that so require, but it is not a cost-effective process. Moreover, wafer bowing due to strain and dissimilar thermal expansion coefficients of GaN and the substrate, leads to difficulties in device layer growth and fabrication.

To achieve high GaN growth rates in vapor phase growth techniques, simple precursors are necessary to achieve high quality growth. For instance, metalorganic precursors used for MOCVD growth are not suitable for high growth rates; the kinetic barrier for the removal of the organic radicals from the metal atom cause high carbon incorporation for high growth rates. Furthermore, to achieve high crystal quality at high growth rates, the growth temperature needs to be sufficiently high. At high temperatures the nitrogen partial pressure over the growing GaN surface is high, which makes a high partial pressure of nitrogen precursor (NH_3 or activated nitrogen) necessary. To achieve this, the growth process can not be performed at vacuum or very low pressure. We believe a suitable range of growth conditions is a total pressure between 0.01 and 1 Bar, and a temperature between 1100°C and 1300°C.

The growth technique investigated in this study was designed specifically to enable the highest possible GaN growth rate. The simplest possible Ga precursor was used, vaporized Ga, thereby eliminating any unnecessary kinetic growth rate limitation.

Furthermore, the Ga vaporization and the growth were performed at atmospheric pressure, which allowed for the use of a high ammonia partial pressure.

To vaporize Ga at high rates into a gas stream at near atmospheric pressures is not trivial. The boiling point of Ga at atmospheric pressure is 2204°C, and the electron-beam evaporation technique commonly used for high temperature evaporation requires high vacuum to function. Assuming a 10% growth efficiency, to reach a growth rate of 1 mm/hr on a 2" wafer, a Ga pure component flow of 0.55 slpm is necessary. Assuming a reasonable gas flow of 5 slpm over a heated Ga source, an 11% Ga concentration in the gas phase is needed, which requires the Ga source to be heated to ~1850°C. To heat a crucible containing Ga to that temperature is difficult in practice; it puts strain on many system components, and reactions between the Ga and the crucible material (typically W or other refractory metal) can be expected.

The main substrate used in the experiments was GaN templates prepared by MOCVD. Material grown on GaN templates was expected to mimic the crystal quality of the template. It was not the purpose of the study to investigate growth on a foreign substrate material, and optimization of the structural quality of the grown crystal. Ultimately, in a production setting the growth would be seeded by GaN substrates previously prepared in the bulk growth system. Alternatively, the first GaN seed could be a small self-seeded crystal obtained in the bulk growth system or obtained from an HVPE system or similar.

Cheap source material were used in the process, solid/liquid Ga and NH_3, and high purities are available. Corrosive gasses such as HCl (used in HVPE) were not utilized, with the potential advantage of limiting hardware corrosion and lowering the gas phase impurities. The operating costs are believed to be low, since the heating in the evaporation cell(s) was localized. Furthermore, due to the widespread use of the related TIG welding technology, the equipment and maintenance cost of the system is believed to be relatively low.

Another advantage of the studied growth technique is that it could be expanded into AlGaN alloys readily. The HVPE technique is presently experiencing problems with Al containing compounds, due to the reactivity of $AlCl_x$ with reactor hardware.

2 Growth System

Figure 1 shows a schematic cross-section of the GaN bulk growth system utilized in the study. The key element in the system is the gallium evaporation cell. An arc discharge is established between a bottom electrode consisting of gallium in a W-crucible, and a top W-electrode positioned above the gallium surface. The gas between the electrodes, and the two electrodes, are heated by the arc discharge to high temperatures. The top W-electrode is water cooled, which, in combination with the relatively high thermal conductivity of W, ensures that the electrode does not melt. The gallium surface forming the lower electrode is heated by the arc, in an area that depends on the geometry of the top electrode and the electrode spacing. The area is on the order of a few millimeters up to a centimeter in diameter. The localized heating at the center of the gallium source causes some gallium to evaporate, and by providing a gas flow perpendicular to the arc the gallium vapor is transported away from the crucible. Downstream from the gallium evaporation cell the gas containing gallium vapors is mixed with ammonia. The mixture is passed between an upper and a lower susceptor heated to a certain growth temperature,

onto which substrates are placed. The gallium vapor reacts with the ammonia to deposit GaN on the substrates.

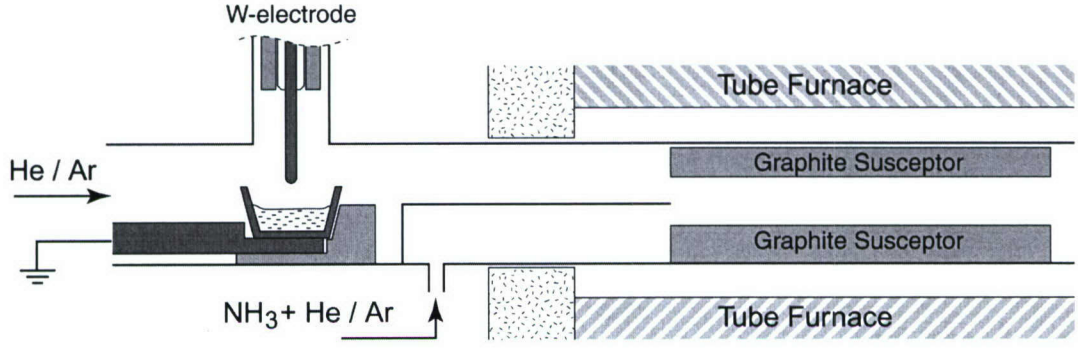

Figure 1. Schematic cross-section of GaN bulk growth system employing gallium arc evaporation.

The W-electrode was mounted in a water-cooled TIG weld torch, which was connected to the negative terminal of a TIG welding generator. The weld torch was modified such that a gas-tight seal could be formed between the torch and the vertical quartz tube providing access to the reactor interior. A stainless steel bellows was also integrated into the torch/quartz fitting, to allow limited vertical movement of the W-electrode. The W-electrode had a 1/8" diameter and a sharp cone-shaped tip, held at a distance of 1/4" – 1/8" from the gallium surface.

The gallium source was placed in a standard Temescal 7cc W-crucible, located beneath the W-electrode. The crucible was seated on a hot-pressed boron nitride support inside the horizontal quartz reactor tube, and was electrically connected to a W-rod, which was connected via a through-feed to the positive terminal of the TIG welding generator. The TIG generator was set to 'straight polarity' (W-electrode = cathode), a configuration that directs ~2/3 of the generated heat into the gallium anode. The arc was started by ionizing the gas for 1-2 sec using the TIG generator's 'high frequency start' feature.

The reactor design resulted in heavy wall deposits, and was not intended for long growth runs. The intention was rather to use this relatively simple reactor vessel to evaluate the basic properties of the growth technique. Issues that needed to be addressed were: Does GaN grow epitaxially on the substrate? Is there spontaneous nucleation of GaN in the gas phase? Are there gallium droplets in the gas phase?

The utilized Ga evaporation technique is similar to several industrial processes in frequent use today. In steel mills, the heat generated by an arc discharge between two or more electrodes is used to melt recycled steel in an arc furnace. Arc evaporation exists as a (near) vacuum process for ceramic coatings. In electro welding, the heat of an arc discharge between a top electrode and a metal surface is used to melt the metal, and in some cases also the top electrode. Particularly the TIG (Tungsten Inert Gas) welding technique is strikingly similar to the utilized Ga evaporation technique, in that the top W-electrode is cooled and is not consumed in the process. Moreover, parallels can be drawn to electron-beam evaporation of metals used in semiconductor device fabrication. In the preferred polarity of the arc discharge, the heating of the Ga surface is caused by electron

bombardment, and the process can therefore be seen as a high-pressure equivalent of electron beam evaporation.

3 Experimental Results

3.1 Gallium Evaporation

First, the characteristics of the arc evaporation cell will be discussed. In argon gas flow, the arc could be established easily using the 'high frequency start' function of the TIG welder. The visible arc was confined to a cone between the tip of the W-electrode and a ~ 5 mm diameter area on the Ga anode. The terminal voltage was typically between 10 and 13 V for the discharge currents used during evaporation. During Ga evaporation fumes could be visible above the Ga surface, and the fumes were subject to the presumably non-laminar gas flow.

With helium gas flow, it was more difficulty to establish an arc using the high frequency start function. Sometimes it was necessary to move the W-electrode into contact with the Ga surface to start the arc. Compared to argon, in helium the visible arc was more diffuse and was not confined to a small area on the Ga anode. The terminal voltage was in the range of 19 to 21 volts during evaporation. There were no visible signs of evaporation present, such as fumes, when evaporating in helium.

With either carrier gas, Ga was successfully evaporated from the W-crucible. During the evaporation the Ga wetted the walls of the W-crucible, but it stayed inside the crucible, and was not visibly contaminated. Once the arc current exceeded a certain value rapid condensation of Ga on the quartz wall above and near the crucible was observed, and it resulted in quick depletion of Ga in the crucible. This put a practical limit on the arc current to 100 A for argon gas, and to 75 A for helium gas.

The fumes that were observed over the Ga surface when evaporating in argon was interpreted as Ga droplets, which is undesirable for high quality growth. Based on this, helium was chosen as the carrier gas for most growths.

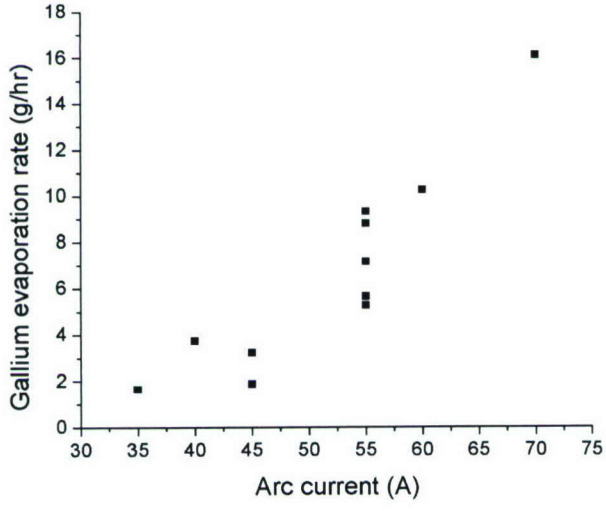

Figure 2. Evaporation rate of gallium vs. discharge current, in helium carrier gas.

The evaporation rate of Ga was measured as the difference in weight of the W-crucible before and after each run. Figure 2 shows data for evaporation rate as a function of the arc current, obtained for various growths performed in helium gas. The expected trend of increased evaporation rate with increasing current can be seen clearly, but it is also evident that the evaporation rate is not fully reproducible. The highest controlled gallium evaporation rate was 16 g/hr.

3.2 Measurement of Upstream Gallium Losses

In the area between the arc evaporation cell and the susceptor, where Ga was transported in the vapor phase before mixing with ammonia, heavy wall deposits were observed during growth. The deposits had a shiny appearance, which suggests a Ga-rich material composition. If a significant portion of the transported Ga was deposited on the walls prior to reaching the susceptor, it would have an adverse effect on the growth efficiency. To quantify the Ga loss, an experiment was performed as illustrated in Figure 3.

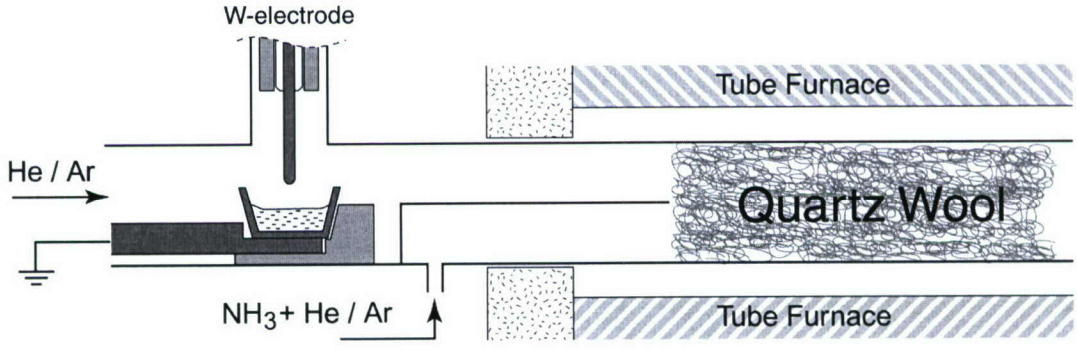

Figure 3. Experiment to measure the loss of Ga in the upper flow channel due to wall deposits.

For identical conditions to GaN growth on substrates located on the susceptors, growth was instead performed in quartz wool that had been placed in the location of the susceptors. The wool was weighed before and after the experiment, and the weight increase was assumed to be of GaN deposited inside the wool. The Ga portion of the deposited GaN was then compared to the amount of Ga evaporated from the W-crucible, and the gallium loss could be calculated. As a check of the method, an experiment was performed at the same conditions but without Ga evaporation, and the change in weight of the wool was found to be insignificant. The stoichiometry of the deposited GaN is unknown, but since Ga is much heavier than N, the error made in assuming stoichiometric GaN deposits inside the wool is small.

Using the described method, the Ga loss was found to be 28 % when using argon as carrier gas, and 76% when using helium as carrier gas.

Wall deposits can be avoided by using a different geometry of the evaporation region and the growth region. The measured loss of Ga is therefore not a big concern, but the information is necessary in order to compare the experimental results to results based on computer flow dynamics simulations.

3.3 Baseline Growth

After exploring the available parameters for the growth of GaN in the reactor, a set of standard conditions were established. The conditions are summarized in Table 1.

Table 1. Conditions and parameters for base-line growth.

Parameter	Value
Carrier gas	He
Total flow	9.3 slpm
Ammonia flow	0.5 slpm
Arc current	55 A
Tube furnace temperature	1160°C
Pressure	1 Atm
Growth time	30 minutes
Substrate	GaN/sapphire MOCVD template

Figure 4 shows photos of samples grown using the base-line conditions. Several pieces of GaN template were loaded in a row to cover the length of the susceptor, with the first piece (left in the picture) flush with the front edge of the susceptor. Samples were loaded in both the top position (underneath the top susceptor) and the bottom position (on the bottom susceptor). The growth in the front ~25 mm of the top samples showed a rough surface morphology, while the growth was specular in the remainder of the top samples. Growth on the bottom samples was dominated by a high density of defects, starting ~20 mm from the front edge. The depositions both on top and bottom samples appeared relatively symmetric side to side about the center line.

To quantify the growth rate, the samples were cleaved along the center (symmetry) line, and the cross sections were examined by scanning electron microscopy (SEM) to determine the film thickness. The film thickness in high defect density areas was measured in smooth areas between the defects. In samples areas where the surface was rough, the film thickness was estimated as an average thickness. The net growth rate was determined by subtracting from the measured GaN film thickness the known thickness profile of the GaN film of the MOCVD template. The growth rate profile thus obtained for a base-line growth has been plotted in Figure 5.

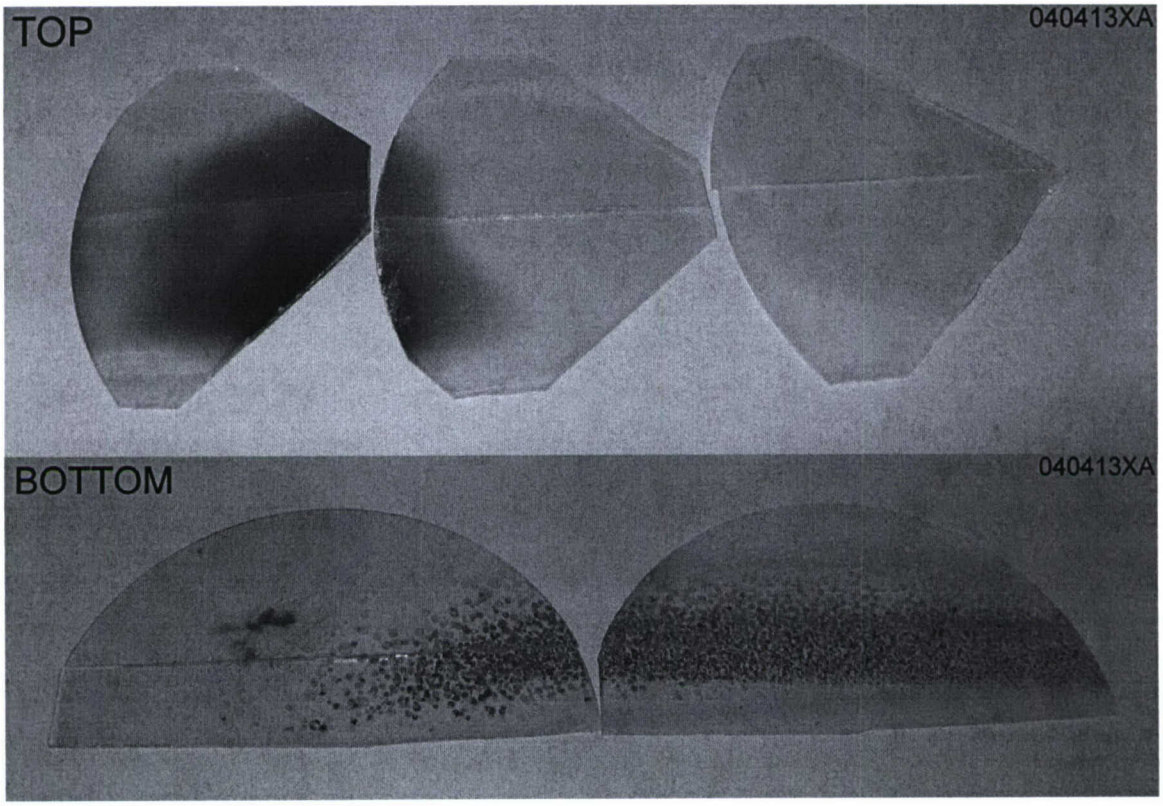

Figure 4. The result of GaN growth on pieces of GaN/sapphire templates using the base-line conditions.

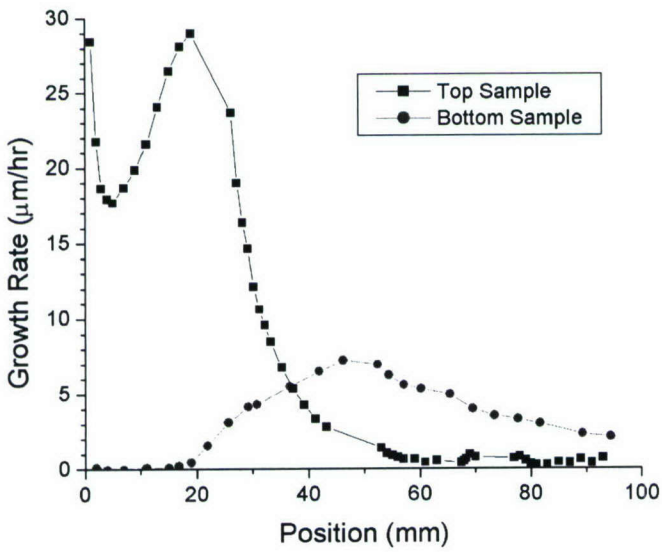

Figure 5. Growth rate as a function of position, measured from the front edge of the susceptor.

3.4 Surface Morphology

Figure 6 (left) shows the atomic force microscopy (AFM) image of a sample after 4μm GaN growth at a growth rate of 16 μm/hr. The right image is the AFM micrograph of the GaN/sapphire MOCVD template used as substrate. The MOCVD template had a poor surface morphology, but after the arc evaporation deposition the GaN surface has recovered and showed step-flow growth.

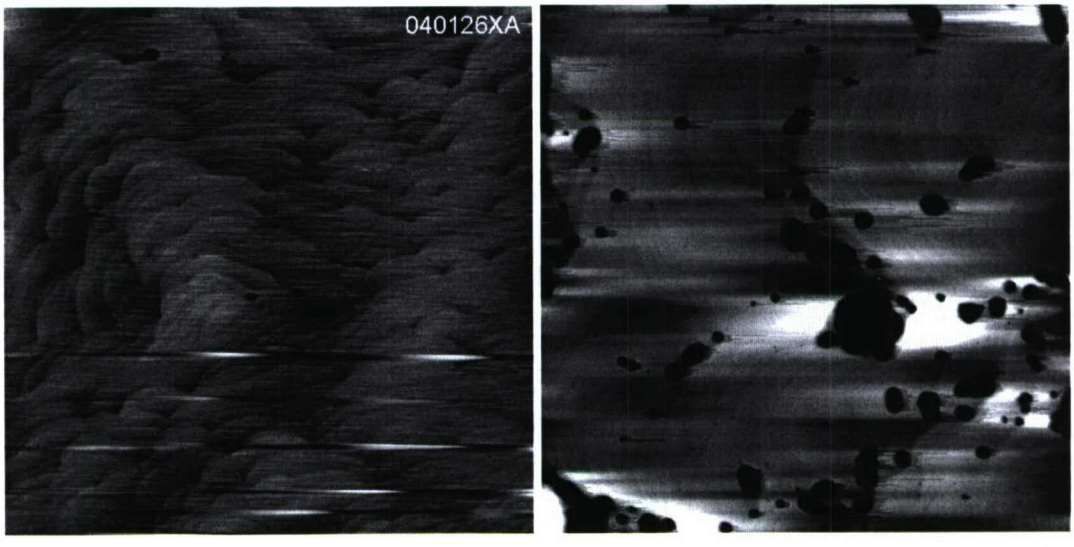

Figure 6. Atomic force microscopy images of GaN deposited by arc evaporation method (left), and GaN MOCVD template used as substrate (right). Scan size is 5μm X 5μm.

3.5 The Effect of Growth Parameters

Figure 7 shows growth rate profiles of samples grown utilizing three different evaporation currents. As can be expected, the average growth rate increased with increasing evaporation current. In the right hand figure, the growth rates have been integrated over the sample length, and are plotted as a function of the gallium evaporation rate. The increase in growth rate with Ga evaporation rate is not fully linear as may have been expected.

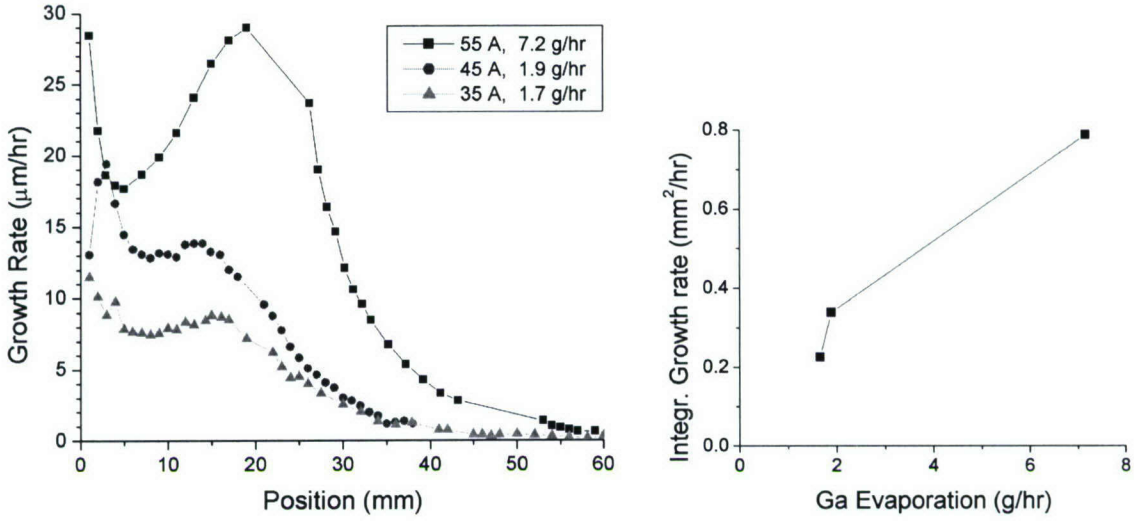

Figure 7. Growth rate profiles for three different arc currents and evaporation rates (left), and the corresponding integrated growth rates *vs.* Ga evaporation rate.

The effect of the ammonia partial pressure was investigated by performing growths where the ammonia flow was varied, while keeping the total flow, and all other parameters, constant. The measured growth rate profiles for three different ammonia partial pressures are shown in the left graph in Figure 8. As the Ga evaporation rate was not stable between the growths, it makes sense for comparison purposes to normalize the growth rates with respect to the Ga evaporation rate for each sample. The right graph in Figure 8 shows the normalized growth rate. The most striking trend is the increase in growth rate with decreasing ammonia partial pressure in the region ~20 mm and beyond the front edge.

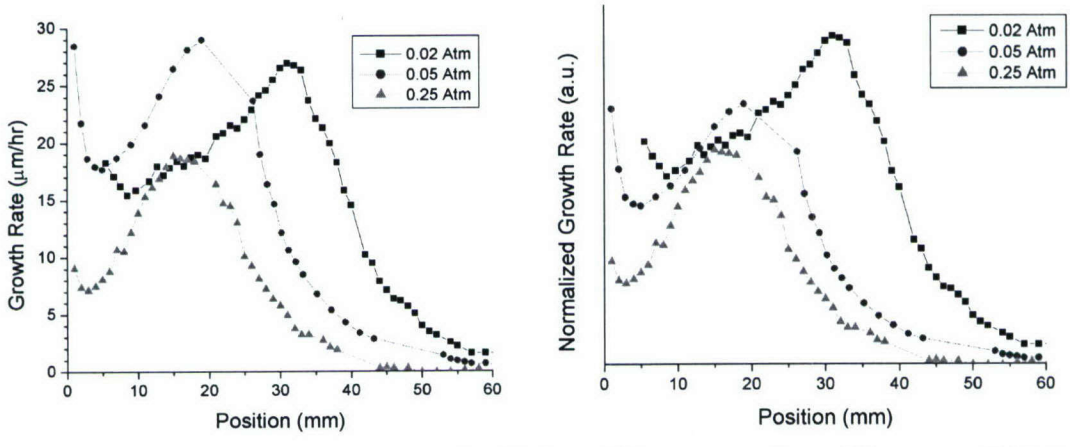

Figure 8. Thickness profiles for growth with three different ammonia partial pressures (left). In the right plot the growth rates have been normalized with respect to the Ga evaporation rate, which provides for a better comparison.

In Figure 9, the growth rate profiles of samples grown in helium and in argon carrier gas have been plotted. In the right plot, for ease of comparison, the growth rates have been normalized with respect to the gallium evaporation rate, and the upstream gallium loss has also been taken into account (see section 3.2).

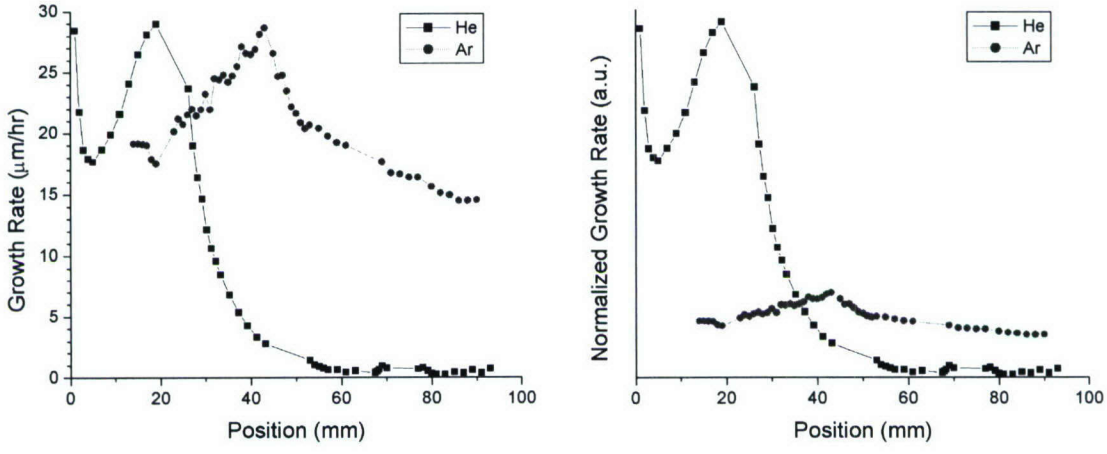

Figure 9. Thickness profiles for growth in argon and helium carrier gas (left). In the right plot the growth rates have been normalized with respect to the gallium evaporation rate, and the difference in upstream gallium loss has also been taken into account.

3.6 Inverted Geometry

As the effect of the arc on the evaporation process was a relatively unknown process, it was desirable to compare growth results with samples utilizing regular thermal evaporation. In the experimental setup, this was achieved by turning the quartz reactor tube up-side down, and removing the boron nitride crucible support, as illustrated in Figure 10. With this geometry, the arc was established between the W-electrode and the W-rod, upon which the W-crucible was located. This served to heat the crucible from underneath.

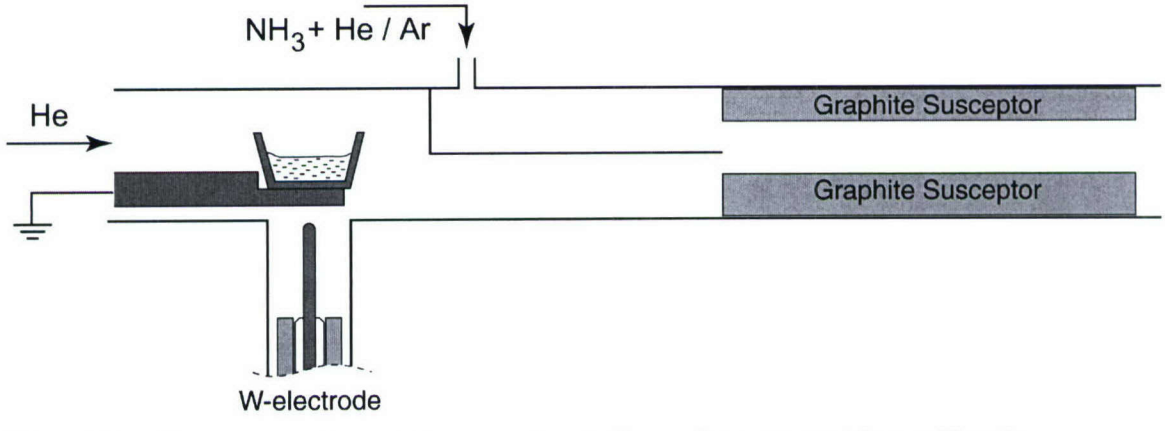

Figure 10. Reactor geometry used for comparison to the regular geometry. Here, gallium is evaporated thermally by heating through the W-crucible.

To achieve evaporation rates similar to the normal geometry, a slightly higher arc current was needed. The resulting growth on samples on the lower susceptor showed much reduced defects compared to the regular geometry, indicating reduced presence of Ga droplets in the gas phase. Figure 11 shows growth rate profiles obtained in the inverted geometry compared to the normal geometry. In the right hand figure the growth rates have been normalized with respect to the gallium evaporation rate. In the plots, the sample loaded on the bottom susceptor in the inverted geometry is plotted together with the sample loaded in the top position in the regular geometry. This makes for a fair comparison, since the sample closest to the group-III inlet is used in both cases. It can be seen that using thermal evaporation does not increase the growth rate in any significant portion of the sample.

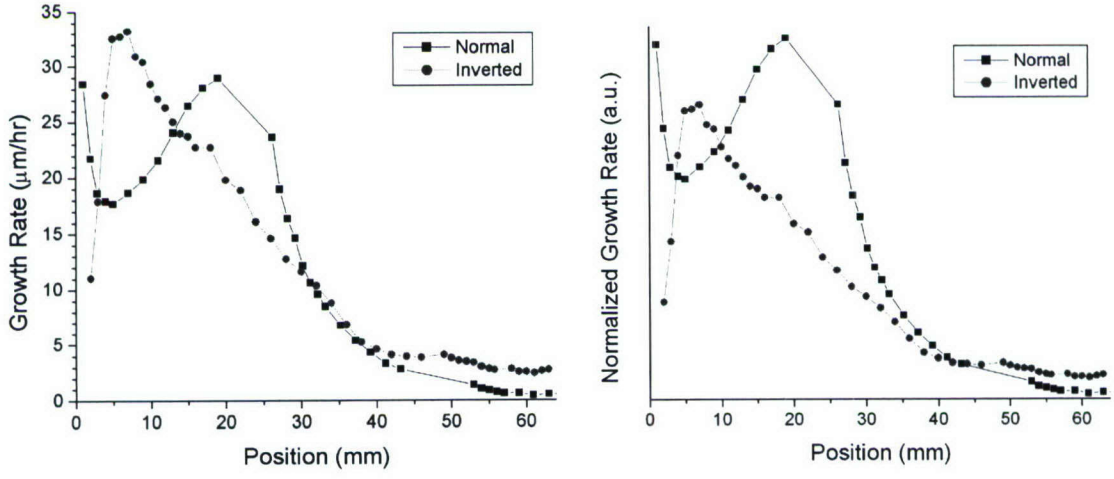

Figure 11. Thickness profiles for samples grown in the normal geometry and the inverted geometry. In the right plot the growth rates have been normalized with respect to the gallium evaporation rate.

4 Analysis & Discussion

4.1 Computer Flow Dynamics Model

As a tool to understand the measured growth rate profiles, and to gauge the efficiency and inherent limitations of the growth technique, computer flow dynamics (CFD) simulations of the reactor were carried out in 3 dimensions using the commercial software package ACE+ from ESI Group (formerly CFDRC). The software allows for multi-physics modeling, including flow, heat transfer, chemistry, and more. A very simple chemistry model was employed, which assumed no gas phase reactions and a sticking coefficient of '1' for Ga on the susceptor. This neglects pre-reactions in the gas phase, and kinetic limitations of the growth rate. The temperature of the susceptor was assumed to be uniform.

The gas parameters used in the CFD simulations were determined as summarized in Table 2. The Lennard-Jones parameters needed for the mix kinetic theory and multicomponent diffusion were taken from the literature. There was some uncertainty in the choice of parameters for Ga species, but we believe the resulting errors are less than

±25%. The gallium concentration in the input flow was based on the measured Ga evaporation rates, with the measured upstream gallium loss factored in (see section 3.2).

Table 2. Methods used to determine parameters for CFD simulations.

Parameter	Method
Gas density	Ideal gas law
Viscosity	Mix kinetic theory
Thermal conductivity	Mix kinetic theory
Mass diffusivity	Multicomponent diffusion

4.2 Modeling Results *vs.* Experimental Results

Figure 12 shows simulated growth rate profiles compared to experimental data, for a base-line growth with He carrier gas, and a comparable growth in Ar carrier gas. The simulated growth rate was high on the upper sample near the front edge, and declined along the length of the susceptor. Conversely, on the lower sample the growth rate started out at zero near the susceptor front edge, and in the case of helium carrier gas increased to levels comparable to the upper growth rate towards the back end of the susceptor. The difference in growth rate between upper and lower susceptors is due to the geometry of the gas inlets. Gallium, the growth rate limiting species, was injected only in the upper half of the gas stream entering the growth zone, and therefore has to diffuse through the lower gas stream to reach the lower susceptor. The diffusion time across the moving gas flow cause a spatial delay in the onset of growth, which was on the order of 15 mm for helium carrier gas. The diffusion rate of gallium in argon is substantially slower, due to the higher molecular weight of argon, and it had the result that the spatial delay in the onset of growth rate exceeded the length of the susceptor.

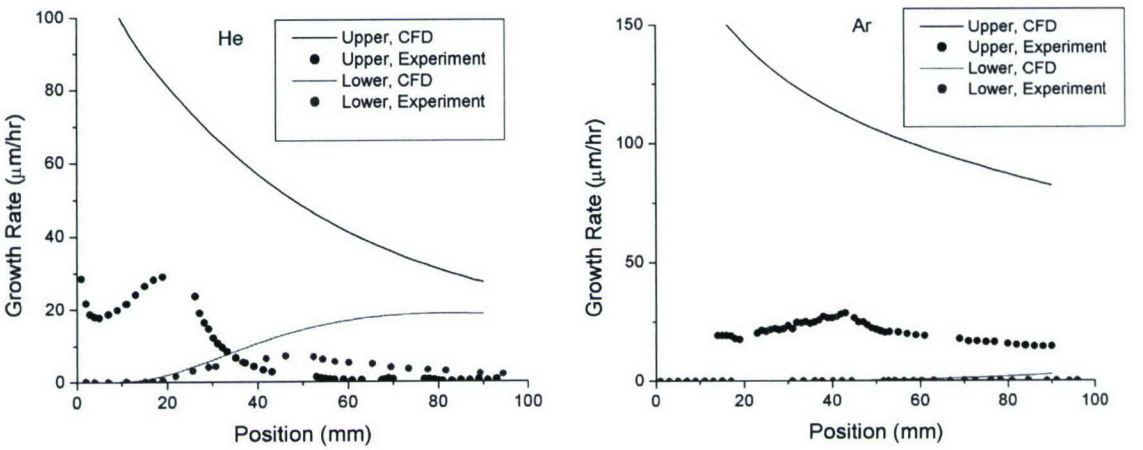

Figure 12. Growth rate profiles simulated by a computer flow dynamics model, for the upper and lower sample position, compared to experimental data. The left figure plots growth rate profiles for the base-line growth, performed in He carrier gas, while the right figure plots growth rate profiles for a growth performed in Ar carrier gas.

The most striking feature in comparing model with experiment is that the growth rate of the upper sample was less than 1/4 of the growth rate predicted in the model, for either carrier gas. For the lower sample grown in He carrier gas, the discrepancy is smaller, but in positions further than ~40 mm from the front edge the experimental growth rate was again very low. There are several potentially important effects that were not included in the simple growth model used in the simulations, and one or more of these could be responsible for the discrepancy. These effects, which will be discussed in the following sections, include Ga-ammonia gas phase pre-reactions, Ga-Ga pre-reactions in the gas phase (droplet formation), and Ga droplet formation in the evaporation cell.

Another significant difference between model and experiment is that the experimental growth rate on the top susceptor typically peaked at a distance of ~20 mm away from the front edge, instead of *at* the front edge. Exceptions to this observations were the growths performed at low Ga evaporation rates (see Figure 7), and the growth performed in the inverted geometry (see Figure 11). The reason for the experimental discrepancy is unclear, but we speculate that it is related to the non-uniform temperature of the susceptor. Since the susceptor was heated by a tube furnace, and the susceptor was located near the front opening of the furnace, it is likely that the relatively cold inlet gas flow has a significant cooling effect on the front part of the susceptor. In the colder part of the susceptor the growth rate could be partially or wholly limited by kinetics of the surface reactions. Experimental support for this idea is the rough surface morphology, a common sign of a too low growth temperature, observed in this area (see Figure 4).

4.3 Gallium – Ammonia Pre-reactions

The experiments showed a strong influence of the ammonia partial pressure on the growth rate (see Figure 8). A reduced ammonia partial pressure resulted in increased growth rates on the upper sample, in the region ~20 mm from the front edge and beyond. One possible explanation of this observed trend is that the flow dynamics of the growth region changed as the ammonia partial pressure was altered. To investigate the effect of ammonia partial pressure in the model, simulations were performed with two different ammonia partial pressures of 0.25 Atm, and 0.05 Atm. The resulting growth rate profiles on the top and the bottom susceptors are shown in Figure 13. It can be seen that the difference in growth rate profile on the upper susceptor is negligible, in comparison to the experimentally observed difference. It can therefore be concluded that changing flow dynamics is not a major reason for the experimentally observed trend.

A more probable explanation is that there are gas-phase pre-reaction involving gallium and ammonia. As the gas-phase concentration of ammonia is lowered, the probability of the Ga-ammonia reaction is reduced, and it leads to lower pre-reaction rates. The role of the pre-reaction product is not clear, but based on pre-reactions observed in MOCVD growth, it appears it does not contribute to the growing film. The pre-reacted molecules are larger and heavier than atomic gallium, which results in reduced diffusion rates and consequently lower growth rates. The molecules may also be kinetically inhibited to partake in the growth process. Moreover, gravity may affect the heavier molecules, reducing the growth rate on the top susceptor. For a given gas velocity, the pre-reaction rate determines the spatial onset of the loss of gallium species, and the decline in growth rate. The experimentally observed lateral extension of the high-growth rate region with

decreased ammonia partial pressure is therefore a direct indicator of pre-reactions involving ammonia.

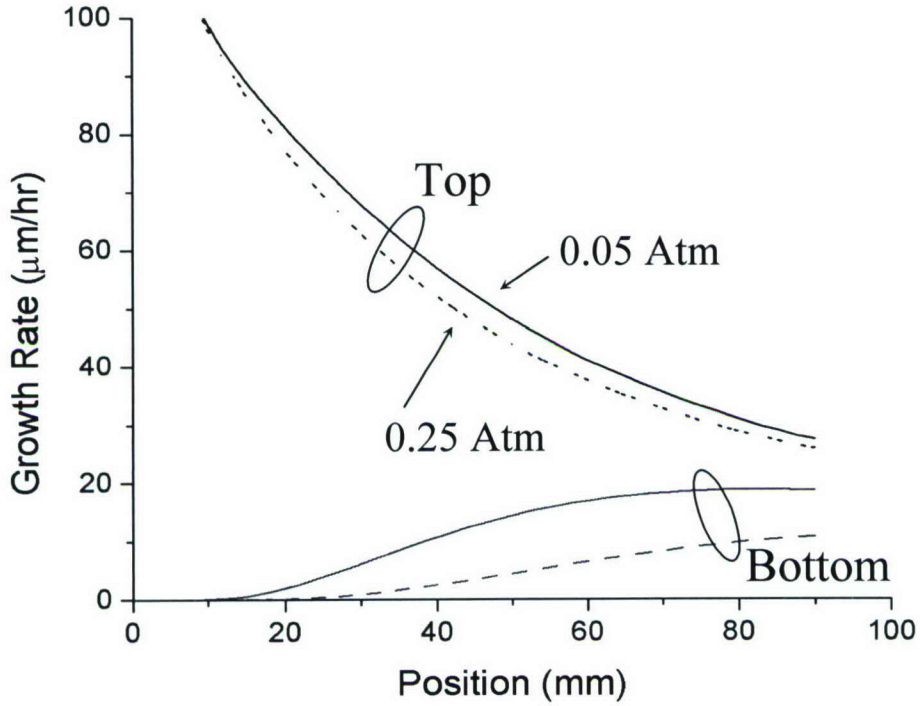

Figure 13. CFD simulations of the growth rate for two different ammonia partial pressures. No significant difference in growth rate on the top sample.

4.4 Gallium Droplets

In the simulation model the gallium species entering the growth zone in the gas phase were assumed to be evenly dispersed as atomic gallium. Considering that the gas temperature and the wall temperature were far below the boiling point of gallium, there is a strong thermodynamic driving force for gallium to condensate, both on walls and in the gas phase. Wall deposits were indeed experimentally observed, and the associated loss of gallium was incorporated into the model.

During the base-line growth in helium, a high density of defects was observed on the lower sample, while none were observed on the upper. This was probably related to the presence of particles or droplets in the gas-phase, responding to gravity. To determine the nature of the observed defects, we consider the thermal evaporation experiment described in section 3.6. In this experiment the defect density on the lower sample was greatly reduced. Pre-reactions with ammonia are likely to be comparable to the base-line process using arc evaporation. This suggests that gallium droplets, and not gallium-ammonia pre-reactions, are the source of the defects. It also indicates that the arc discharge process evaporates gallium not only in atomic form, but also in droplets. This problem is similar to particle problems commonly encountered in other arc-evaporation deposition techniques.

The gallium droplets forming defects on the lower sample reduces the amount of gallium in the gas phase available for growth, and consequently reduces the growth rate.

However, this reduction is low and it is not a concern for the efficiency of the growth technique. This can be concluded from Figure 11, where the sample grown by thermal evaporation, with a low defect density, does not have a higher growth rate than the regular sample. The droplet formation is rather a concern from a material quality standpoint, but the problem can be circumvented for instance by using a vertical reactor design.

Gallium droplet may form not only during evaporation, but also by Ga-Ga interaction in the gas phase. Very high gas temperatures exist in the evaporation arc, and it can easily support large gallium concentrations in the gas phase. As the hot gas is mixed with the colder main gas stream, the gas containing the Ga vapor cools off, and this can lead to gas-phase condensation. The size of the droplets would be smaller than those causing macroscopic growth defects, as these were found to be related to the evaporation process. Whether or not gas-phase condensation is a significant effect can not be concluded from the experimental data.

4.5 Growth Efficiency

To obtain the total growth efficiency for the base-line growth, the growth rate profiles for the top and the bottom samples were integrated along the length of the susceptor. The obtained values were then multiplied by the available width of the susceptor (26 mm). The resulting volume growth rates were 20.5 mm^3/hr and 8.6 mm^3/hr, for the upper and lower sample positions, respectively. The total growth rate, 29.1 mm^3/hr, corresponds to a deposited weight of 0.177 g/hr of GaN. The Ga portion of the weight rate, 0.147 g/hr, was divided by the measured Ga evaporation rate of 7.2 g/hr, and resulted in an efficiency of 2.0 %. This value is probably an overestimate, since the calculations assume a growth profile that is uniform side-to-side.

The low efficiency is due in part to features specific to the reactor design that can be avoided with improved designs. The Ga loss due to wall condensation upstream of the growth zone is one such feature, and if removed, it would result in a growth efficiency of around 8 %. The Ga loss due to ammonia pre-reactions was severe, and it can only be addressed by reducing the residence time of the mixed species in the hot zone, or further reducing the ammonia partial pressure. The residence time can be improved by lowering the total reactor pressure.

5 Conclusions

The studied growth technique was found capable of growing high quality gallium nitride on MOCVD GaN templates. Growth rates as high as 30 μm/hr were demonstrated. The surface morphology of the sample area close to the susceptor front edge was rough, presumably due to a low susceptor temperature caused by gas cooling. In the smooth sample areas the surface shows step-flow growth by AFM.

The experiments showed that the growth technique has potential, as well as inherent limitations. The fact that reasonable results were achieved in a simple reactor at the first attempt, suggests that with more development work the technique can be greatly improved. Potential advantages of the technique are cheap source materials of high purity and low operating costs due to the localized heating of the evaporation cell(s). Since no

corrosive gasses are used, hardware corrosion can be reduced, which leads to reduced gas phase impurities. Furthermore, due to the widespread use of the related TIG welding technology, the equipment and maintenance cost of the system is believed to be relatively low.

The low growth efficiency observed in the experiments is probably the largest obstacle for the technique to become commercially useful. Some improvement can be had by redesigning the reactor geometry, but the high gallium-ammonia pre-reaction rate is an inherent limitation. Theory predicts that the pre-reactions can be reduced by lowering the total reactor pressure, but this could not be verified experimentally, since the reactor was not equipped with a vacuum system and pressure control.

5.1 Future Work

The simple growth system used in the study was sufficient for proof of concept, and to study some of the basic growth properties. To further gauge the potential of the growth technique, a more elaborate growth system would be needed. Following are a few features that would be of interest to study:

- Growth at reduced reactor pressure, to reduce gallium-ammonia pre-reaction. The effect of the reduced pressure on the properties of the arc discharge would also need to be characterized.
- Vertical geometry of the evaporation zone and the growth zone. This would allow gallium condensation on the walls to flow back into the gallium crucible and be recycled.
- Hot wall design of region upstream of growth zone, including the evaporation zone. By allowing the inlet gas stream to heat up before entering the evaporation zone, and remaining hot until reaching the growth zone, gallium droplet formation may be reduced.
- Use of He/H_2 mixture or pure H_2 gas for carrier gas and arc discharge medium. H_2 would dissociate in the discharge and recombine downstream creating heat, to prevent gallium droplet formation or gas phase nucleation.
- Long term stability of the evaporation cell. Look for degradation of the W-electrode and the W-crucible.